Surfactant modulated interactions of hydrophobically modified ethoxylated urethane (HEUR) polymers with penetrable surfaces

Mervat S. Ibrahim[a,b], Stephen King[c], Martin Murray[d], Agnieszka Szczygiel[d], Bruce D. Alexander[a], and Peter C. Griffiths[a]

[a] Faculty of Engineering and Science, University of Greenwich, Medway Campus, Chatham Maritime, Kent ME4 4TB, UK

[b] Pharmaceutics Department, Faculty of Pharmacy, Modern Sciences and Arts University (MSA), 26 July Mehwar Road intersection with Wahat Road, Cairo, Egypt

[c] Science and Technology Facilities Council, ISIS Facility, Rutherford Appleton Laboratory, Didcot, Oxfordshire OX11 OQX, UK

[d] AkzoNobel, Wexham Road, Slough, Berkshire, SL2 5DS, UK

Corresponding Author

Peter Griffiths

Email: P.Griffiths@greenwich.ac.uk

Telephone: +44(0)208 331 9927

Keywords: HEUR, SDS, PGSE-NMR, and SANS.

Abstract

Hypothesis

Adsorption of hydrophobically modified ethoxylated urethane polymers (HEURs) at the soft colloid interfaces of emulsion droplets will stabilise oil-in-water emulsions (a) *via* steric stabilisation induced by adsorption of the polymer at the droplet surfaces through the hydrophobic groups, and (b) *via* continuous phase viscosity enhancement through polymer self-association. Both of these mechanisms will be modulated by the presence of the surfactant, sodium dodecylsulfate (SDS).

Experiments

Dodecane-in-water emulsions stabilised by three HEUR polymers with different structural composition were examined in the absence and presence of SDS by NMR spectroscopy and small-angle neutron scattering (SANS). The effect of adsorption of the polymer to the dodecane droplet surfaces, and the conformation of the self-associating polymer in the aqueous solution were quantified.

Findings

All emulsions were stable for days-weeks. Diffusion data showed the formation of oil droplets of hundreds of nm in size in the presence of all three HEURs, here denoted C_6-L-(EO_{100}-L)$_9$-C_6, C_{10}-L-(EO_{200}-L)$_4$-C_{10}, and C_{18}-L-(EO_{200}-L)$_7$-C_{18}, where EO_x represents a block of ethylene oxide of x monomers, L denotes the linker group, and C_n the length of the hydrophobic end-group. No significant changes in droplet size

across this series of polymers was observed. Collectively, the results point to adsorption of the polymer to the droplet surfaces, which results in a small decrease in the effective polymer solution concentration, thereby driving to significant changes in the structure and dynamics of the system. Evident in the SANS data in particular, is a subtle balance between the characteristic features reflecting polymer self-association, and those associated with polymer structures commensurate with a larger length-scale, dependent on the system composition. Surprisingly, the polymer and polymer/SDS complex in the presence of oil show slightly *greater* diffusive rates relative to the analogous systems in the absence of the oil.

Finally, the partitioning of the three polymers in phase-separated samples was studied by ^{1}H NMR, and it was shown that the C_{18}-L-$(EO_{200}$-L$)_{7}$-C_{18} exhibited a greater partitioning in the oil phase compared with C_{6}-L-$(EO_{100}$-L$)_{9}$-C_{6} and C_{10}-L-$(EO_{200}$-L$)_{4}$-C_{10}, an observation that may be understood in terms of the structural composition of the HEURs. The SDS showed a positive correlation between its partitioning in the two layers with the polymer partitioning, evidence of a strong interaction between the surfactant and the polymer, consistent with the behaviour observed in the oil-free system.

Introduction

Emulsions are commonly used in the personal care industry to minimise the undesirable “greasy feel” of actives and emollients (oils), which can be a negative attribute for the consumer. By dispersing such oils in an aqueous environment, the sensory perception can be altered to make it more favourable to consumers. Emulsions often contain surfactants in conjunction with thickeners to provide stability of the two phases *via* control of the viscosity. Although there are a variety of rheological modifiers available in the personal care industry, there is a desire for shorter formulation lists, which in turn drives the need for multifunctional additives. Here, we explore whether hydrophobically modified ethoxylated urethane polymers (HEURs) could function as such an additive.

Emulsions are commonly stabilised by surfactants (1–3), proteins (4,5), hydrocolloids (6) and particles (7–9). To date, few studies have attempted to stabilise emulsions or microemuslions with hydrophobically modified water soluble polymers. Filali *et al.* studied the network structure of hydrophobically poly(ethylene oxide) (PEOM) PEOM-10-12 (the first number is the molecular weight of the polymer in kg mol^{-1} and the second number is the hydrophobic end-group length) in decane/water microemulsions by small-angle neutron scattering (SANS) (10). The decane microemulsion is pre-stabilised by cetylpyridinum chloride (CPCl) and octanol (co-surfactant), before the addition of the PEOM. The oil droplet radius was constant (62 ± 2 Å) for the various concentrations of decane (7 - 26 %). The scattering analysis of the microemulsion data indicate spherical droplets, from which the radius of the oil droplet is calculated. It is postulated that the hydrophobic end-groups of the polymer tend to adsorb to the oil, and as the volume fraction (φ_v) of the oil increases, the distance (d) between the

droplets becomes comparable to the polymer radius of gyration (R_g), and the polymer tends to form bridges between the droplets.

Bagger-Jorgensen *et al*. studied the diffusion of PEOM-11-18 in decane emulsions pre-stabilised by penta(ethylene glycol) monododecyl ether ($C_{12}E_5$) (11). The oil concentration was held constant with weight fraction, φ_w = 0.2, and the polymer concentration varied from 0.002 < φ_w < 0.02. The self-diffusion coefficient of the polymer measured by NMR decreases in the presence of the oil droplet, suggesting the adsorption of the polymer hydrophobic end-groups to the oil droplets. When the parent PEO was added to the decane emulsion, no change in the diffusion coefficient of the polymer in the emulsion is noted, and therefore the polymer does not adsorb to the droplets. The neutron scattering from the emulsion as a function of PEOM concentration could also be interpreted in terms of a sphere form factor of radius 72 ± 2 Å. The variation of the polymer concentration does not affect the size of the oil droplet but a change in the *inter*-droplet distance was observed. The increase in the polymer concentration leads to an increase in an attractive force, hence the distance between the droplets decreases. Bagger-Jorgensen, in agreement with Filali *et al.* (10), postulates that the PEOM hydrophobes adsorb to the oil droplets, where some polymer chains bridge between two droplets with the PEO backbone extended in water.

Causse *et al* used Pluronic L64 (poly(ethylene oxide)–poly(propylene oxide)–poly(ethylene oxide)), (EO_{13}–PO_{30}–EO_{13}), to stabilise tributylphosphate (TBP)/water emulsions (12). The concentration of the Pluronic was held constant at 10 wt% and the oil concentration varied. The microemulsions were studied by SANS, and the scattering curves were fitted to a core-shell model. Increasing the oil content increases the hydrophobic core radius whereas the shell thickness was constant (35 Å).

Stieber *et al.* studied water/octane microemulsions stabilised by a triblock PEO-hydrophobic polyisoprene copolymer using static and dynamic light scattering (13). Two diffusion coefficients were observed for the polymer stabilised microemulsion, a fast diffusion coefficient (3×10^{-11} $m^2 s^{-1}$), and a range of slow diffusion coefficients (1×10^{-12} to 1×10^{-14} $m^2 s^{-1}$). Increasing the polymer concentration didn't result in any change in the fast diffusing component, whereas the slow diffusion got slower. The fast diffusion might be explained by the collective droplet diffusion. The slow diffusion is correlated to the adsorbed polymer chain onto the oil droplets where the polymer chains tend to bridge between two droplets and larger aggregates are formed. The diffusion coefficient of the same system was measured by diffusion NMR and similar conclusions are reported by Struis *et al.* (14).

The effects of SDS on PEOM stabilised emulsions have not been reported extensively, however, homopolymer stabilised emulsions have been studied. A mixture of polymer and surfactant has proved to provide better stabilising effect than polymer or surfactant alone where PVP (neutral polymer) and SDS were used to stabilise 30 % xylene/5mM SDS/PVP emulsions where the SDS concentration was held constant at 5 mM and the PVP concentration was varied ($0.01 < \varphi_w < 0.2$ wt%). This may be explained by adsorption of the polymer/surfactant complex on the oil droplet which provides two stabilising mechanisms - steric and electrostatic. The stability of the emulsion was assessed by counting the droplet concentration where an increasing number of droplets reflects better stability of the particles (15).

In this paper, a particular focus is on the ability of three HEURs with different structural composition to adsorb to oil droplets, with this adsorption being explored in the absence and presence of SDS. A correlation with emulsion stability, and a comparison with the polymer/surfactant solution interaction is made.

Materials and methods

Materials

Sodium dodecylsulfate (SDS) (Aldrich, no impurity observed in surface tension data), deuterated sodium dodecylsulfate (d_{25}-SDS) (ISIS deuteration facility), dodecane (Aldrich, ≥ 99 %), d_{26}-dodecane (Aldrich, ≥ 98% D), deionized water (Purite Select deionizer) and deuterium oxide (D_2O) (Aldrich, purity 99.9%) were used as received. The HEUR polymers, gifts from Dow, as discussed previously (21), had average structures C_6-L-$(EO_{100}$-L$)_9$-C_6, C_{10}-L-$(EO_{200}$-L$)_4$-C_{10} and C_{18}-L-$(EO_{200}$-L$)_7$-C_{18}, where L is the urethane linker, EO_x is a monomer unit ethylene oxide block with x monomers and a $C_{6,10,18}$ are alkyl end-groups. As is inevitable with such commercial samples, it is expected that these polymers will exhibit a range of heterogeneity, both structural and molecular weight, but one that does not lead to unsurmountable challenges when being analysed by diffusion NMR (21).

Methods

The emulsions were prepared by probe sonication of solutions comprising 5 or 20 wt% dodecane in the presence of a range of SDS and polymer concentrations (Hielscher UP 40 st ultrasonic processor, 5 min).

Nuclear Magnetic Resonance techniques

High-resolution ^1H Nuclear Magnetic Resonance

The emulsions were prepared in D_2O. These experiments were designed to detect the concentration of polymer, dodecane and SDS in the phase-separated emulsions of

polymer/dodecane and polymer/SDS/dodecane mixtures. The intensity of component-specific peaks were integrated relative to an external probe (chloroform), loaded in a coaxial insert in the samples. The same coaxial insert was used in all sets of samples to ensure the same concentration of chloroform was detected each time. Experiments were carried out at 25 °C on a 400 MHz Bruker FT NMR spectrometer. A simple 90° pulse-acquire NMR sequence was used, averaging 4 scans with a recycle delay of at least 5 times the spin−lattice relaxation time between consecutive scans.

Pulsed-Gradient Spin-Echo Nuclear Magnetic Resonance (PGSE-NMR)

Polymer/dodecane and polymer/dodecane/SDS mixtures were prepared in D_2O, experiments were carried out at 25 °C on a 400 MHz Bruker FT NMR spectrometer.

A stimulated echo sequence was used, in which the diffusion time (Δ) was set to 800ms, the duration (δ) of the gradient pulses was held constant to 1 ms and their intensity (G) varied from 5 - 800 G cm^{-1}. Typically, 16 scans were accumulated over 32 gradient steps. Self-diffusion coefficients were extracted by fitting the peak intensities (I) to Equation 1 for the peaks at 3.75 ppm (EO), 4 ppm (SDS) and 1 ppm (dodecane and SDS), where I_0 is signal intensity in absence of gradient pulses, D_s the diffusion coefficient, γ the gyromagnetic ratio of protons (16,17).

$$\mathrm{I} = \mathrm{I}_0\, e^{-D_s\gamma^2 G^2 \delta^2 \left(\Delta - \frac{\delta}{3}\right)} \qquad \text{Equation 1}$$

Peak overlap often requires analysis *via* double exponentials or CORE analysis (23), but here, the intensity of the dodecane peak far outweighed that of SDS so the more complex fitting approach was not needed.

Neutron Scattering

SANS measurements were carried out at 25°C on the LOQ diffractometer (ISIS spallation Neutron Source, Oxfordshire, UK). Neutrons wavelengths spanning 2.2-10 Å were used to access a Q range of 0.0008 to 0.25 $Å^{-1}$ ($Q = 4\pi \sin(\theta/2)/\lambda$) (18) with a fixed sample-detector distance of 4.1 m. Temperature control was achieved through the use of a thermostatted circulating bath pumping fluids through the base of the sample changer, which allowed the experiment to run at 25 ± 0.5 °C. Samples were contained in UV-spectrophotometer grade 1 mm path length quartz cuvettes (Hellma). The scattering data were normalized for the sample transmission and the incident wavelength distribution, corrected for instrumental and sample backgrounds using a quartz cell filled with D_2O (this also removes the incoherent instrumental background arising from vacuum windows), and corrected for the linearity and efficiency of the detector response using the instrument specific software package. The data were put onto an absolute scale using a well characterised, partially deuterated polystyrene blend standard sample. The intensity of the scattered radiation, $I(Q)$, as a function of the wave vector, Q, is given by Equation 2;

$$I(Q) = N_p V_P^2 \Delta\rho^2 P(Q) S(Q) + B_{inc} \qquad \text{Equation 2}$$

where N_p is the number and V_p the volume of the scattering species, $\Delta\rho$ the difference between the neutron scattering length density (SLD) of the scattering species and the solvent, *P(Q)* describes the morphology of the scattering species, *S(Q)* describes the spatial arrangement of the scatterers in solution, and B_{inc} is the incoherent background.

Results and discussion

Emulsions stabilised by three HEUR polymers of different hydrophobicity have been studied and compared. In the context here, stability is defined as a constant droplet size for at least three days, but phase separation may occur on a longer time scale. The diffusion coefficients of the polymer and dodecane were both quantified to characterise the oil droplet size and to contrast the relative key interactions in this three-component mixture (HEUR/SDS/dodecane). A series of contrast match SANS experiments were conducted to identify the scattering from the polymer or polymer/SDS complexes in HEUR/dodecane and HEUR/SDS/dodecane mixtures, to give information about any adsorbed polymer layer on the oil droplet, in presence and absence of SDS. The phase separated emulsions were studied to track the equilibrium partitioning of the polymers, SDS, and dodecane between the oil and aqueous phase, and to explore any correlations with the hydrophobicity of the polymer, and any preferential interaction of the polymer with SDS.

Diffusion NMR analysis of the emulsion

In the absence of SDS, the diffusion NMR data indicates that the dodecane droplets have the same average diffusion coefficient in the presence of the three studied polymers, Figure 1. The decays of the dodecane signals followed Equation 1 over a wide range of signal intensity, indicating that any polydispersity in the droplet size has been smeared out by fast exchange of the dodecane between the droplets. Further, the diffusion data are mutually similar but slightly faster in the presence of SDS, except for the C_6-L-(EO_{100}-L)$_9$-C_6/SDS complex. Clearly, polymer hydrophobicity has little

effect on the size of the droplet formed, and the presence of the SDS has only a subtle effect on the droplet diffusion (size), except in the C_6-L-(EO_{100}-L)$_9$-C_6 case.

These HEUR polymers self-associate in aqueous solution and form complexes with SDS (21), that lead to significant and complex sample-dependent changes in the dynamics (viscosity, diffusion) and structure of the system. In the presence of *penetrable* interfaces, adsorption of the polymer hydrophobic end-groups to the droplet surface is likely to induce changes in the polymer network structure, these being reflected in the measured average polymer diffusion coefficients (no signature of interface-bound polymer was observed in the attenuation functions, so it is assumed that fast exchange is operating) and in the scattering profiles.

It has been shown in previous work that the HEURs adopt a sparse network structure below the polymer critical overlap concentration as a result of the connection of flower micelles into clusters (19), and thus the average diffusion rate $\langle D_s \rangle$ follows;

$$\langle D_s \rangle = \sum_{i=1}^{n} p(i) D_s(i) \qquad \text{Equation 3}$$

where *i* represents each of the *n* different environments that the polymer (free molecule, flower micelle, cluster, network, and by extention to this study, droplet bound) may exist in, with population *p(i)* and self-diffusion coefficient $D_s(i)$ respectively.

Fast exchange allows is to consider, conceptually, the relative diffusion coefficient (D_r) of the polymer is presented, defined as $D_r = \frac{D_{polymer\ in\ emulsion}}{D_{polymer\ solution}}$, where $D_{polymer\ solution}$ is the polymer diffusion coefficient in the simple aqueous polymer solution. As such, changes in the D_r value reflect perturbation of the polymer network structure – through changes in *i, p(i)* and $D_s(i)$ – induced by the presence of the oil.

For all three polymers, $D_r > 1$, Figure 2, indicating that the polymer is *more mobile* in the presence of the emulsion droplet. Ostensibly contradictory, the presence of larger, more slowly diffusing droplets has the effect of *increasing* the mobility of the polymer. One explanation for this could be a shorter residence time of the polymer hydrophobes within the polymer network in the presence of the oil droplet. Put differently, the oil droplet perturbs the polymer network structure, effectively diluting the solution polymer phase and thereby, weakening the network structure. The observed increases in polymer self-diffusion coefficient are commensurate with a decrease in polymer network strength consistent with a few tenths of % drop in concentration, not inconsistent with the mass of polymer that might be present at the droplet surface.

In presence of SDS, bearing in mind that the SDS interacts with the polymers (20), an analogous ratio may be defined, SDS *viz*, $D_r = \frac{D_{polymer\ in\ emulsion}}{D_{polymer+SDS\ solution}}$. Again, one might infer that if the D_r values for the polymer in the HEUR/SDS/dodecane mixture approach unity, the polymer/SDS interaction is more favoured than the polymer/dodecane one. As may be seen, the D_r values for the polymer in the emulsion are only slightly larger than unity, Figure 2, typically 1.2 – 1.5.

Inferences drawn from the diffusion data – that the network structure is altered by a small effective decrease in polymer concentration - were tested by exploring the conformation of the polymer and polymer/surfactant complex in solution and the emulsions using SANS.

SANS analysis of the polymers in the emulsion

Three different contrast variation SANS experiments have been carried out to characterise the emulsions formed from the three polymers. The data are presented as a *3x3* composite matrix in Figure 3, with each polymer as a column and the three experiments as the rows. Within each panel, different scattering curves are presented reflecting the concentration points studied. The ensuing discussion focuses largely on the gross features in the data, with the analysis presented in the Supplemental Section.

In the first row, SANS is collected for aqueous h-polymer/d-dodecane (surfactant-free) emulsions, for each polymer, where the scattering length density (SLD) of the d-dodecane was "matched" to the solvent using a mixture of D_2O (92 %)/H_2O; hence, the observed scattering arises *only* from the polymer. A second set of experiments - presented in the second row - were carried out with aqueous h-polymer/h-SDS/d-dodecane emulsions in 92% D_2O, where the scattering contribution is from the polymer/SDS complex. Finally, in the third experiment – third row - the scattering from aqueous h-polymer/d-SDS/d-dodecane emulsions in 92 % D_2O was measured, where again only the polymer contributes to the scattered intensity, but in this case, in the ternary mixture. A comparison of these three experiments should allow the impact of the droplet and the droplet *plus* SDS on the polymer conformation to be assessed.

Selected data are presented here, with additional experiments contained in the Supplemental Section.

We have previously examined these polymers in aqueous solution (21) and adsorbed to impenetrable surfaces (22), in the absence and presence of SDS. Across these distinct sets of systems, the scattering patterns show significant similarities and some notable differences. Focus first, on the gross differences, the biggest of which pertains to the greatly reduced intensity of the shoulder/peak observed in the solution scattering around Q=0.03 Å, that feature ascribed to self-associated structures through the aggregation of the polymer hydrophobes. The second most notable difference is a significant increase in the scattered intensity at low-Q in the emulsion systems, commensurate with a larger length-scale, interpreted as polymer adsorption to the droplet surfaces.

Several models to describe these sets of data (polymer coils, solid spheres, core-shell structures, simple adsorbed layer) were tested but all were found to be deficient in some manner – the fit had the wrong shape, or couldn't reproduce all the features in the data. However, a complex composite model built on the solution scattering modelling (21) shows universal applicability so has been developed further here;

$$I(Q) = I(Q)_1 \left\{ \frac{4}{3}\pi R^3 \frac{(sin(QR) - QRcos(QR))}{(QR)^3} S(Q) \right\} + \left\{ \frac{I(Q)_2}{(1+Q^2\xi^2)} \right\} + \left\{ \frac{I(Q)_3}{(1+Q^2A^2)^2} \right\} + B_{inc}$$

Equation 4

The first component in the model, with intensity $I(Q)_1$, is a solid sphere to reflect the SDS / polymer hydrophobic aggregate (given that the oil droplet size is too big to be detected in the experimental window probed here). The structure factor S(Q) of the sphere is represented by the charge on the SDS micelle (or HEUR/SDS mixed micelle). The second component – a polymer network – considers two correlation length-scales;

a Lorentzian length (ξ) with intensity $I(Q)_2$, which reflects the fluctuation in the polymer network structure, a Debye-Bueche length (A) with intensity $I(Q)_3$, reflecting the length-scale associated with the larger network formed by the polymer, and one can associate this term with any adsorbed polymer layer.

Depending on the contrast, and the various concentrations, all three terms may not be needed in order to yield an acceptable fit to the data. Practically, when fitting such neutron data, and in the absence of complimentary contrast data that precludes simultaneous fitting, insensitivity of the fit to one component within the composite model is interpreted as that component not being needed *i.e.* the "best" model is one that fits the data with the fewest parameters. Broadly speaking, however, the two length-scale model is required for the polymer/surfactant case at low surfactant concentrations, with the second length-scale becoming more significant with increasing surfactant or oil, and ultimately, the micellar term is required for the highest surfactant concentration systems studied.

Return to the gross features in the data. In the polymer-only scattering contrast recorded for C_6-L-(EO_{100}-L)$_9$-C_6/dodecane mixtures, the intensity of the polymer scattering increases - as expected - as a function of polymer concentration, Figure 3 (a), top panel, and the shoulder observed at Q = 0.02 and 0.03 Å for 2 and 5 wt%, respectively, Figure S.1, is lost in the presence of the dodecane droplet, Figure 3 (a), top panel. In addition, the intensity increases significantly at low-Q on addition of dodecane, which may be explained by the presence of the polymer associated with dimensions commensurate with larger aggregates. Both facts indicate adsorption of the polymer on the oil droplet (21), most likely through the hydrophobic moieties.

With increasing (*on-match*) droplet concentration, the scattered intensity from the polymer showed no change in intensity or position of the mid Q feature (Q=0.03A). However, the scattering pattern showed a significant decrease at low Q in the presence of low concentrations of droplets, which, ultimately, resembles the characteristic pattern of the simple polymer. One concludes that with increasing polymer concentration (or *inter alia*, decreasing droplet concentration), the surfaces become saturated and the polymer adopts a structure more closely resembling the solution one (whether SDS is present or not).

Examining the detail in the data and its modelling, consider the scattering of the C_6-L-(EO_{100}-L)$_9$-C_6/SDS in presence of 20 wt% dodecane, Figure 3 (a), middle row. With increasing SDS concentration, the scattered intensity at low-Q increases and ultimately, micelle-like scattering is observed at Q = 0.07 Å for the highest concentration value, 1 wt% SDS. The key parameters that represent these fits are presented in Table S.1. The micellar term (spherical, 18 Å) is necessary only at the higher SDS concentrations. The Lorentzian length and its intensity decrease as a function of increasing SDS concentration, whereas the Debye-Bueche length and its intensity increase. The increase in the Debye-Bueche term reflects the emergence of larger structures commensurate with the strengthening of the network around the droplets. Similar conclusions may be drawn from the C_{10}-L-(EO_{200}-L)$_4$-C_{10} and C_{18}-L-(EO_{200}-L)$_7$-C_{18} polymers, Figure 3 (b) and (c) middle panel, and Tables S.2 and S.3, respectively.

In the final series of experiments on polymer/d-SDS/d-dodecane mixtures, the scattering again arises only from the polymer, Figure 3 bottom row. There are subtle changes at low-Q as a function of SDS concentration in all three sets of polymer scattering, with the effect most noticeable in the C_6-L-(EO_{100}-L)$_9$-C_6 case, Figure 3(a).

The fitting parameters are presented in Table S.4. Here, the parameters show similar changes in the network length-scales as the polymer/SDS contrast, however, the intensities of these terms are slightly lower. Similar conclusions may be drawn from the C_{10}-L-$(EO_{200}$-L$)_4$-C_{10} and C_{18}-L-$(EO_{200}$-L$)_7$-C_{18} polymers, Figure 3 (b) and (c) and Tables S.5 and S.6, respectively.

Further comparisons on the gross features may be drawn. Comparing Figure 3 with Figure S.2 reveals that varying the dodecane concentration imparts only very subtle changes on the polymer scattering. There is an increase in the intensity at low-Q in the presence of dodecane, Figures S.3-4, the magnitudes of which are dependent on the specific polymer, but seem to increase with the level of hydrophobicity of the polymer. The increase in the scattered intensity is reflective of the formation of bigger aggregates, quantified through the Debye-Bueche term. Similar conclusions may be drawn from the C_{10}-L-$(EO_{200}$-L$)_4$-C_{10} and C_{18}-L-$(EO_{200}$-L$)_7$-C_{18} cases, Figures S.3 and S.4, Tables S.7 and 8, respectively.

Such conclusions are consistent with previous studies. Filali *et al.*, presented scattering data for PEOM adsorbed to pre-stabilised decane emulsions as a function of oil concentration. In their studies, they observed changes in the scattered intensity at low-Q, reflective of an attractive interaction (10). Varying the level of oil in the emulsions had a very subtle effect, which lends support to the hypothesis drawn from their diffusion data of the presence of free polymer at 5 wt% dodecane, where the 0.5 wt% polymer is able to stabilise the dodecane in water up to 20 wt%.

^{1}H NMR studied for the phase separated emulsions

Emulsions stabilised by 0.5 wt% HEUR/SDS/20 wt% dodecane were left to phase separate (> weeks) into an oil top layer and an aqueous bottom layer. Samples from the two layers were transferred to NMR tubes and the ^{1}H NMR integrals of the polymer, SDS, and dodecane peaks were determined relative to an external chloroform calibrant, Figure S.5. As exemplar, the integrals are presented in Table 1 for the aqueous phase and Table 2 for the oil phase in presence of C_6-L-(EO_{100}-L)$_9$-C_6. The values of the polymer, SDS, and dodecane integrals relative to the chloroform peak give information on the partitioning of the polymer, SDS, and dodecane in the two layers of the phase separated emulsion. The integration of the C_{10}-L-(EO_{200}-L)$_4$-C_{10} and C_{18}-L-(EO_{200}-L)$_7$-C_{18} polymers in presence of SDS are presented in Tables S.5 and S.6 for the aqueous layer and Tables S.7 and S.8 for the oil layer.

The polymer partitioning in the three-component mixture polymer/SDS/dodecane is higher in the aqueous phase for the C_6-L-(EO_{100}-L)$_9$-C_6, C_{10}-L-(EO_{200}-L)$_4$-C_{10}, whereas C_{18}-L-(EO_{200}-L)$_7$-C_{18} shows higher partitioning in the oil layer, a clear reflection of the hydrophobicity of the polymers. The SDS partitioning is higher in the aqueous phase in presence of C_6-L-(EO_{100}-L)$_9$-C_6 and C_{10}-L-(EO_{200}-L)$_4$-C_{10} whilst in presence of C_{18}-L-(EO_{200}-L)$_7$-C_{18} the SDS partitioning is higher in the oil phase. The dodecane concentration in the aqueous phase is very low, but increasing the SDS concentration enhances the solubilisation of dodecane in the aqueous phase. Therefore, the SDS has a synergistic solubilising effect to the polymer. The SDS/polymer interaction is present evidenced by the direct correlation between polymer and SDS partitioning in the aqueous and oil phase.

Conclusions

Three different HEUR polymers denoted C_6-L-(EO_{100}-L)$_9$-C_6, C_{10}-L-(EO_{200}-L)$_4$-C_{10}, and C_{18}-L-(EO_{200}-L)$_7$-C_{18} were used to stabilised dodecane/water emulsions in the absence and presence of SDS. These hydrophobically modified water soluble polymers possess a multifaceted character, and potentially, offer a route to stabilising novel emulsions with optimised formulations for challenging or high value cargoes [*e.g.* 24-26]. Interestingly, the structural composition / hydrophobicity of the polymers and the addition of SDS had only very subtle effects on the size of the oil droplet formed. The scattering data showed evidence of steric stabilisation of the oil droplet through polymer adsorption, and a decrease in the polymer network structure. All data were well-described by a composite model embodied in two length-scale for the polymer, and a micellar term at higher surfactant concentrations. Changes in the intensities for these two terms, and their lengths, were consistent with an evolution of the dominating polymer environment from an adsorbed polymer layer to a self-associated network with coexisting droplets, reflective the competing roles of the polymer. Phase separated emulsion studies showed a direct correlation between the polymer and SDS partitioning in the aqueous and oil layers - as the polymer concentration increases in each layer, there is a commensurate increase in the SDS concentration. The architecture of the polymers affected the polymer partitioning in the two layers of the phase separated emulsions where the C_{18}-L-(EO_{200}-L)$_7$-C_{18} showed higher partitioning in the oil layer whereas the C_6-L-(EO_{100}-L)$_9$-C_6, and C_{10}-L-(EO_{200}-L)$_4$-C_{10} favoured the aqueous layer, consistent with their effective hydrophobicity. Insights from this study will hopefully direct the future design of multifaceted formulation components.

Figures

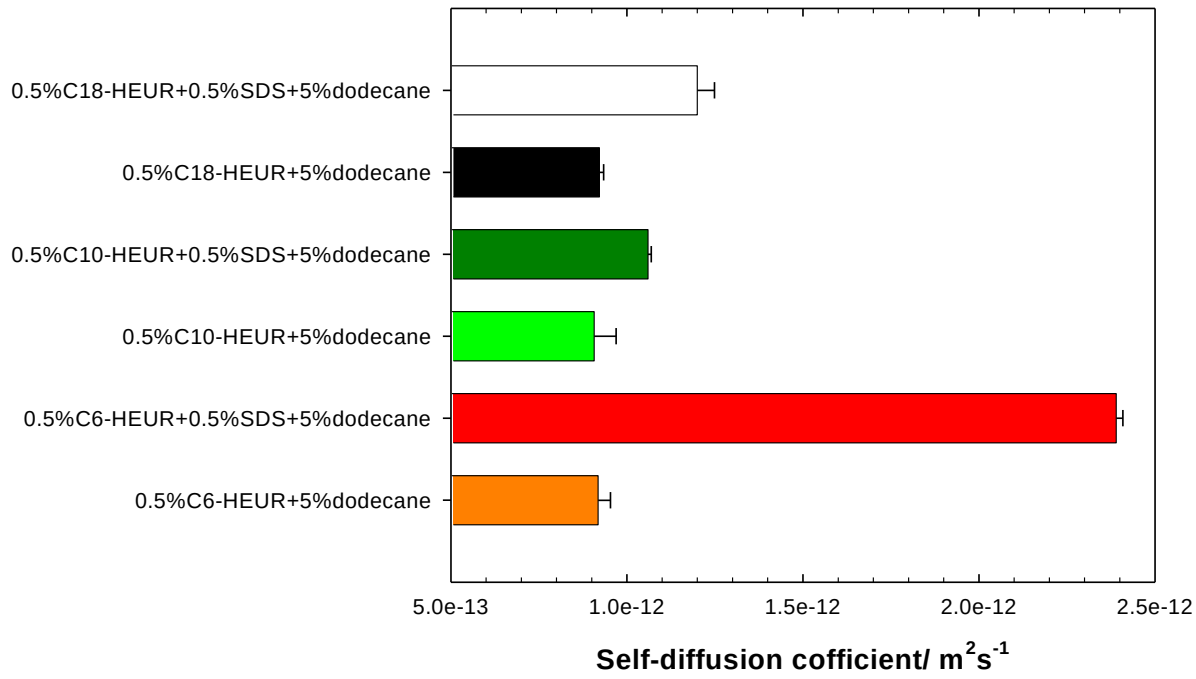

Figure 1. Average self-diffusion coefficients of dodecane in polymer/dodecane and polymer/SDS/dodecane mixtures, for the three polymers studied here C_6-L-(EO_{100}-L)$_9$-C_6 (C_6-HEUR), C_{10}-L-(EO_{200}-L)$_4$-C_{10} (C_{10}-HEUR), and C_{18}-L-(EO_{200}-L)$_7$-C_{18} (C_{18}-HEUR). Average values were determined from three discrete measurements.

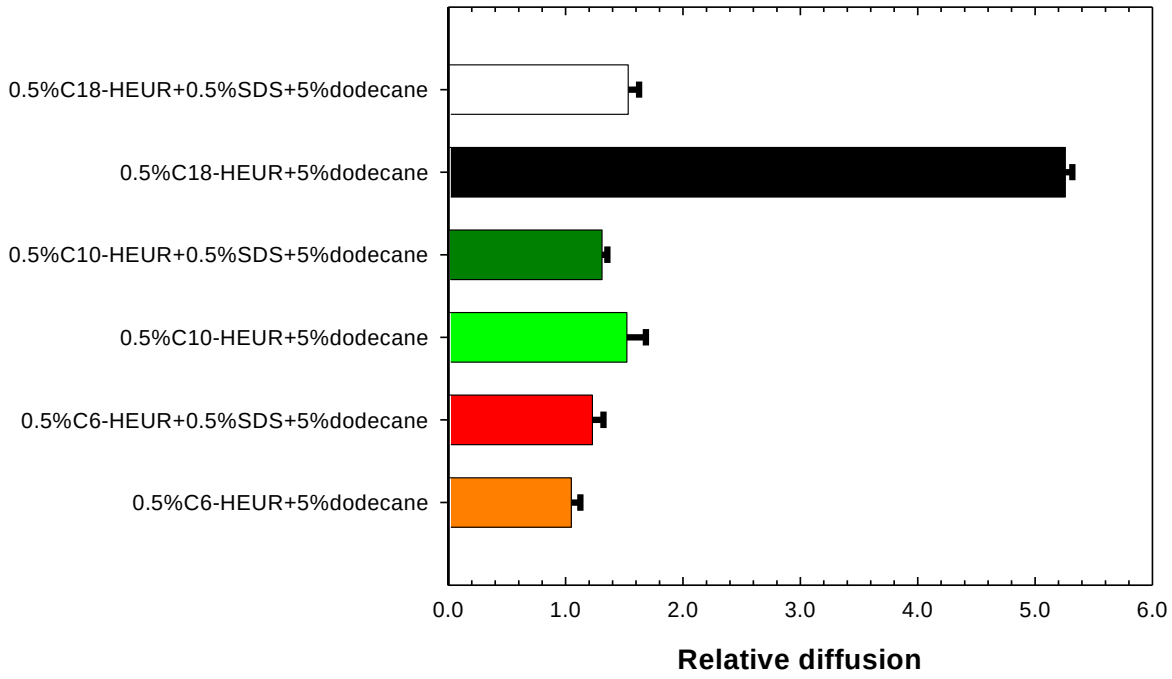

Figure 2. Relative average self-diffusion coefficients of C_6-L-(EO_{100}-L)$_9$-C_6 (C_6-HEUR) , C_{10}-L-(EO_{200}-L)$_4$-C_{10} (C_{10}-HEUR), and C_{18}-L-(EO_{200}-L)$_7$-C_{18} (C_{18}-HEUR) in polymer/dodecane and polymer/SDS/dodecane mixtures. Average values were determined from three discrete measurements.

(a)

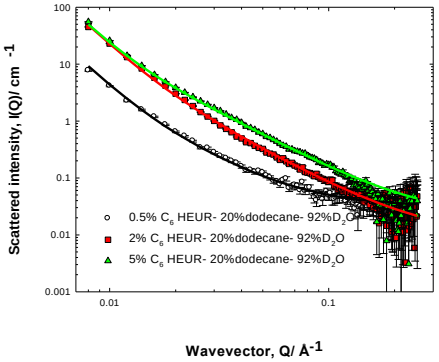
Scattered intensity, I(Q)/ cm -1
Wavevector, Q/ Å-1
0.5% C6 HEUR- 20%dodecane- 92%D2O
2% C6 HEUR- 20%dodecane- 92%D2O
5% C6 HEUR- 20%dodecane- 92%D2O

(b)

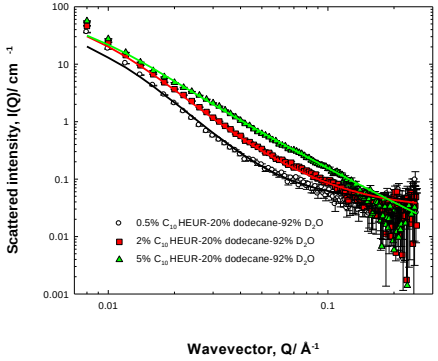
Scattered intensity, I(Q)/ cm -1
Wavevector, Q/ Å-1
0.5% C10 HEUR-20% dodecane-92% D2O
2% C10 HEUR-20% dodecane-92% D2O
5% C10 HEUR-20% dodecane-92% D2O

(c)

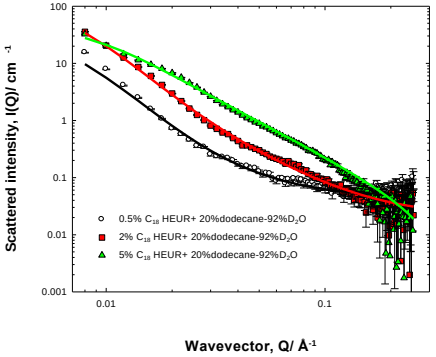
Scattered intensity, I(Q)/ cm -1
Wavevector, Q/ Å-1
0.5% C18 HEUR+ 20%dodecane-92%D2O
2% C18 HEUR+ 20%dodecane-92%D2O
5% C18 HEUR+ 20%dodecane-92%D2O

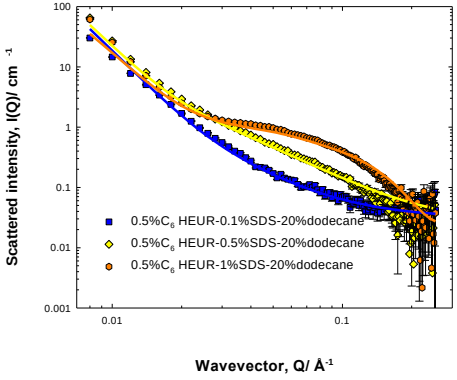
Scattered intensity, I(Q)/ cm -1
Wavevector, Q/ Å-1
0.5%C6 HEUR-0.1%SDS-20%dodecane
0.5%C6 HEUR-0.5%SDS-20%dodecane
0.5%C6 HEUR-1%SDS-20%dodecane

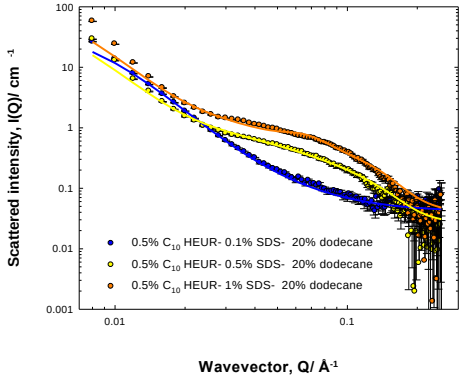
Scattered intensity, I(Q)/ cm -1
Wavevector, Q/ Å-1
0.5% C10 HEUR- 0.1% SDS- 20% dodecane
0.5% C10 HEUR- 0.5% SDS- 20% dodecane
0.5% C10 HEUR- 1% SDS- 20% dodecane

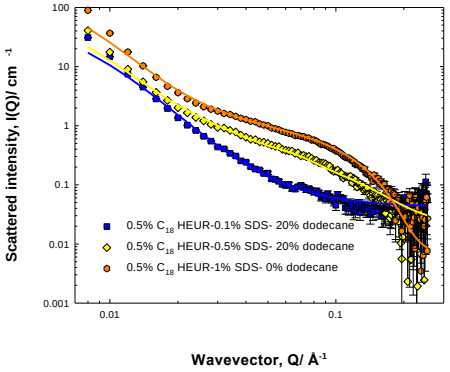
Scattered intensity, I(Q)/ cm -1
Wavevector, Q/ Å-1
0.5% C18 HEUR-0.1% SDS- 20% dodecane
0.5% C18 HEUR-0.5% SDS- 20% dodecane
0.5% C18 HEUR-1% SDS- 0% dodecane

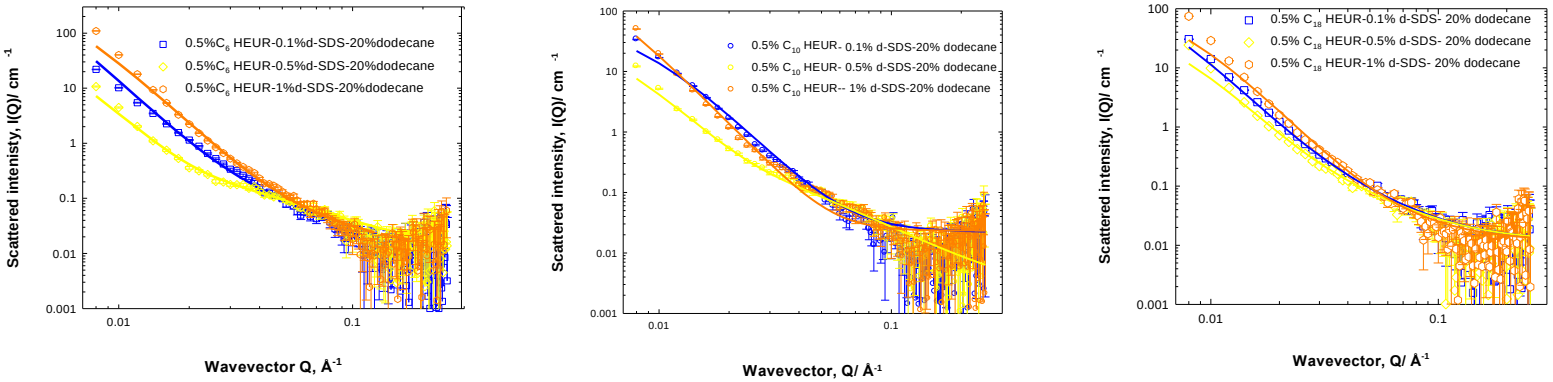

Figure 3. Comparison of SANS from h-polymer/d-dodecane (20 wt%) mixtures (panel in top row) at various polymer concentrations; 0.5 (white circles), 2 (squares), and 5 (triangles) wt% for the three polymers studied here (a) h-C_6-L-(EO_{100}-L)$_9$-C_6 (b) h-C_{10}-L-(EO_{200}-L)$_4$-C_{10} (c) h-C_{18}-L-(EO_{200}-L)$_7$-C_{18}. Middle row panel, SANS from h-polymer/h-SDS/d-dodecane at various SDS concentrations 0.1 (squares), 0.5 (diamonds), and 1 (hexagons) wt%, where polymer and dodecane concentrations are fixed at 0.5 and 20 wt%, respectively. Bottom row panel SANS from h-polymer/d-SDS/d-dodecane at the same polymer, SDS, and dodecane concentrations as the middle panel. Samples were prepared in 92 %(v/v) D_2O to match the SLD of d-dodecane to the solvent. Measurements were carried out at 25 °C. The solid lines in column (a) graphs are fits for sphere and network model.

Sample	Chloroform	SDS ± 0.2	Polymer ± 0.2	Dodecane ± 0.2
5 % SDS/0.5 % polymer	1	6	7	121
3 % SDS/0.5 % polymer	1	3	5	41
1 % SDS/0.5 % polymer	1	1	5	14
0.1 % SDS/0.5 % polymer	1	n.d.	3	8

Table 1. Integration of C_6-L-(EO_{100}-L)$_9$-C_6, SDS and dodecane peaks relative to the chloroform (external probe) peak in aqueous layer of phase separated emulsions.

Sample	Chloroform	SDS ± 0.2	Polymer ± 0.2	Dodecane ± 0.2
5 % SDS/0.5 % polymer	1	4.5	4.5	250
3 % SDS/0.5 % polymer	1	3	5.5	60
0.5 % SDS/0.5 % polymer	1	n.d.	5.5	300
0.1 % SDS/0.5 % polymer	1	n.d.	6	6800

Table 2. Integration of C_6-L-(EO_{100}-L)$_9$-C_6, SDS and dodecane peaks relative to the chloroform (external probe) peak in oil layer of phase separated emulsions.

Figure 3 – individual figures

Top row

(a)

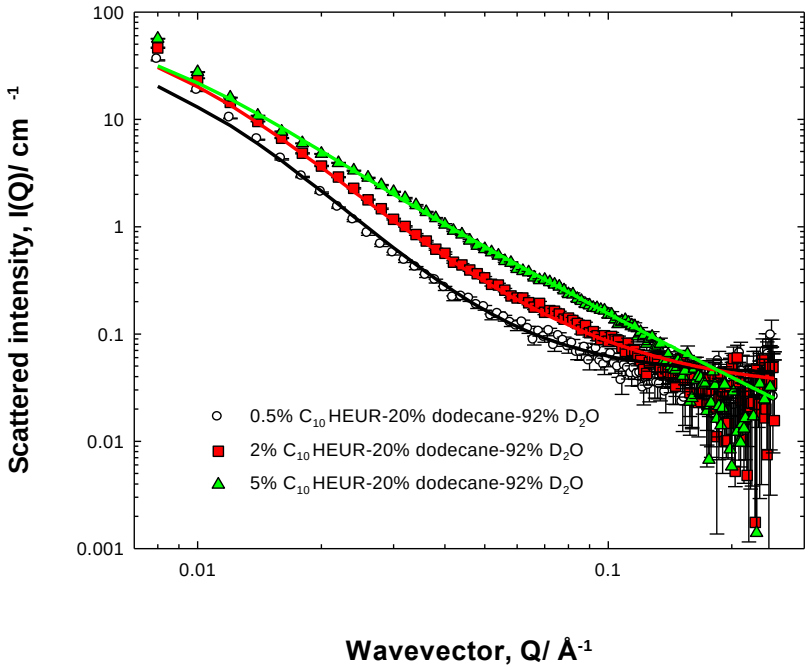

(b)

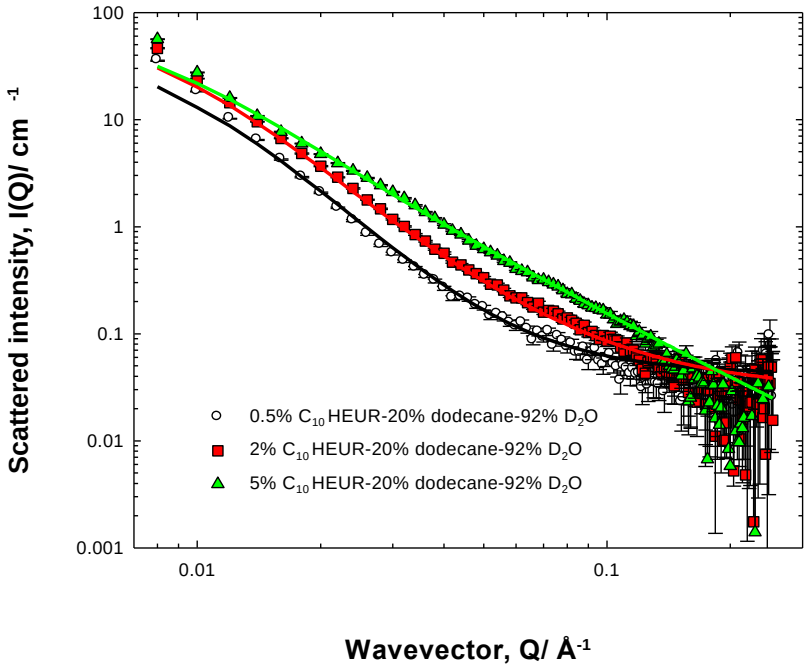
Scattered intensity, I(Q)/ cm -1
100
10
1
0.1
0.01
0.001
0.01
0.1
0.5% C10HEUR-20% dodecane-92% D2O
2% C10HEUR-20% dodecane-92% D2O
5% C10HEUR-20% dodecane-92% D2O
Wavevector, Q/ Å-1

(c)

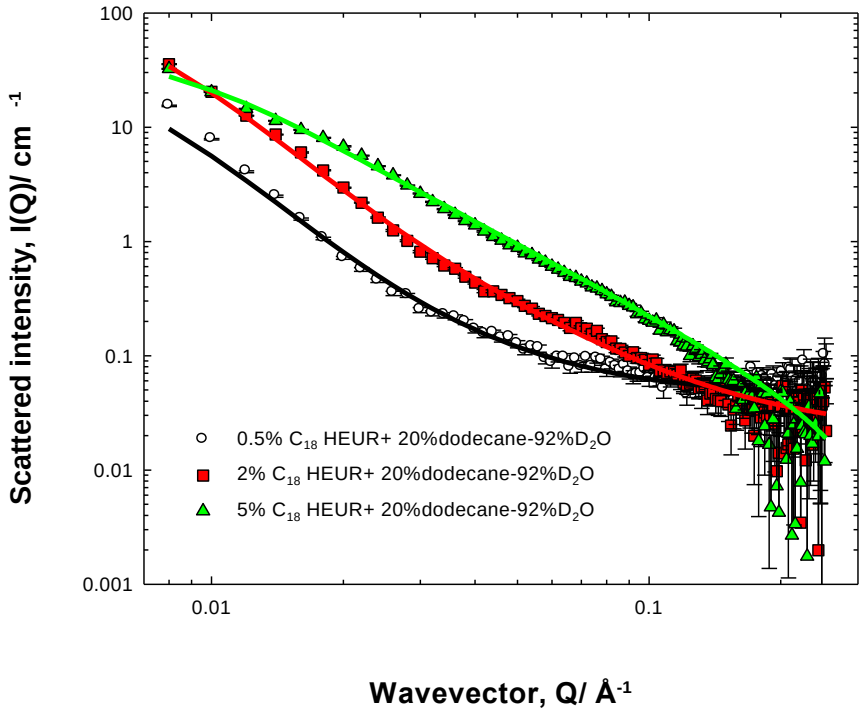
Scattered intensity, I(Q)/ cm -1
100
10
1
0.1
0.01
0.001
0.01
0.1
0.5% C18 HEUR+ 20%dodecane-92%D2O
2% C18 HEUR+ 20%dodecane-92%D2O
5% C18 HEUR+ 20%dodecane-92%D2O
Wavevector, Q/ Å-1

Middle row

(a)

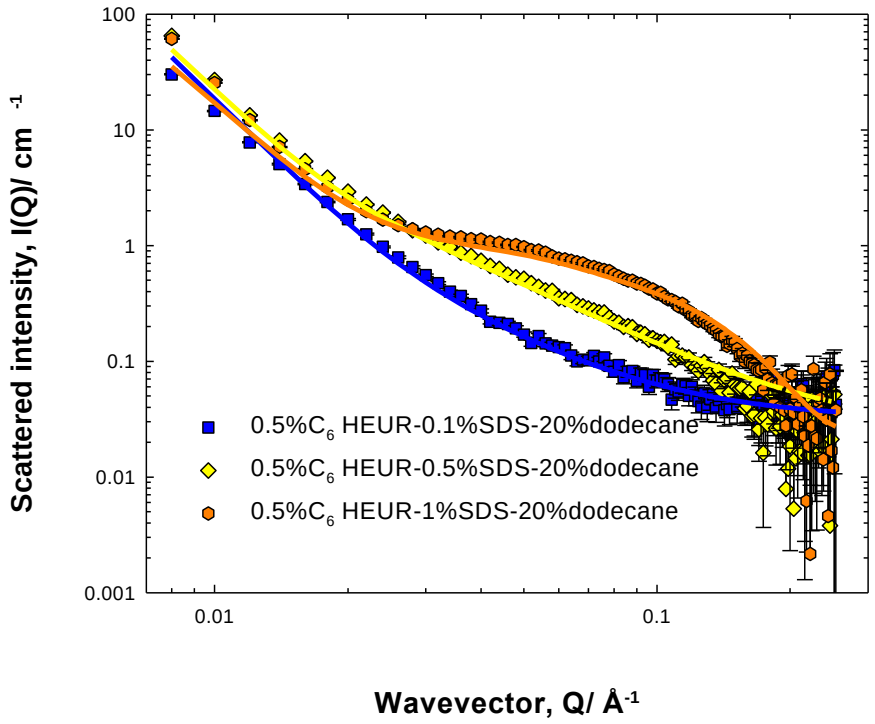
100
10
1
0.1
0.01
0.001
0.01
0.1
Scattered intensity, I(Q)/ cm -1
Wavevector, Q/ Å-1
0.5%C6 HEUR-0.1%SDS-20%dodecane
0.5%C6 HEUR-0.5%SDS-20%dodecane
0.5%C6 HEUR-1%SDS-20%dodecane

(b)

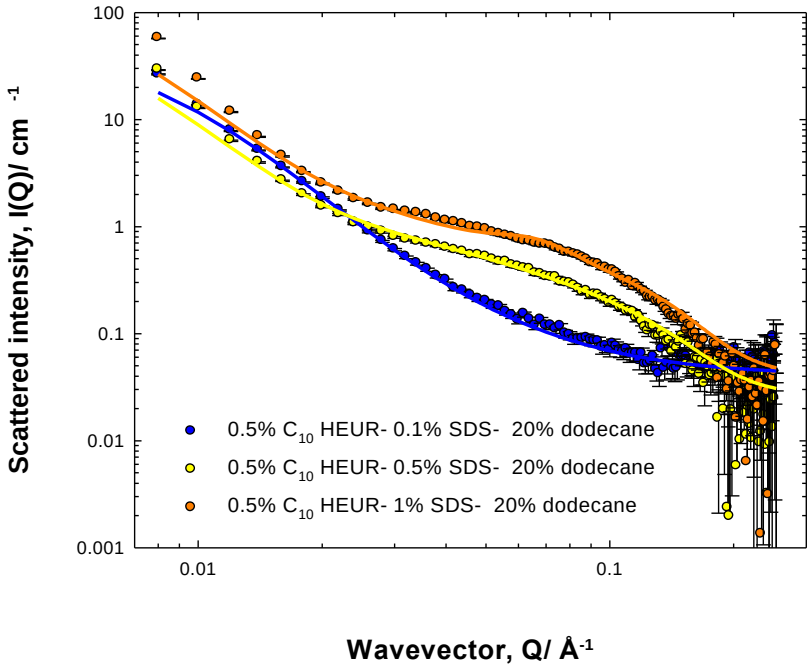
Scattered intensity, I(Q)/ cm -1
100
10
1
0.1
0.01
0.001
0.01
0.1
0.5% C10 HEUR- 0.1% SDS- 20% dodecane
0.5% C10 HEUR- 0.5% SDS- 20% dodecane
0.5% C10 HEUR- 1% SDS- 20% dodecane
Wavevector, Q/ Å-1

(c)

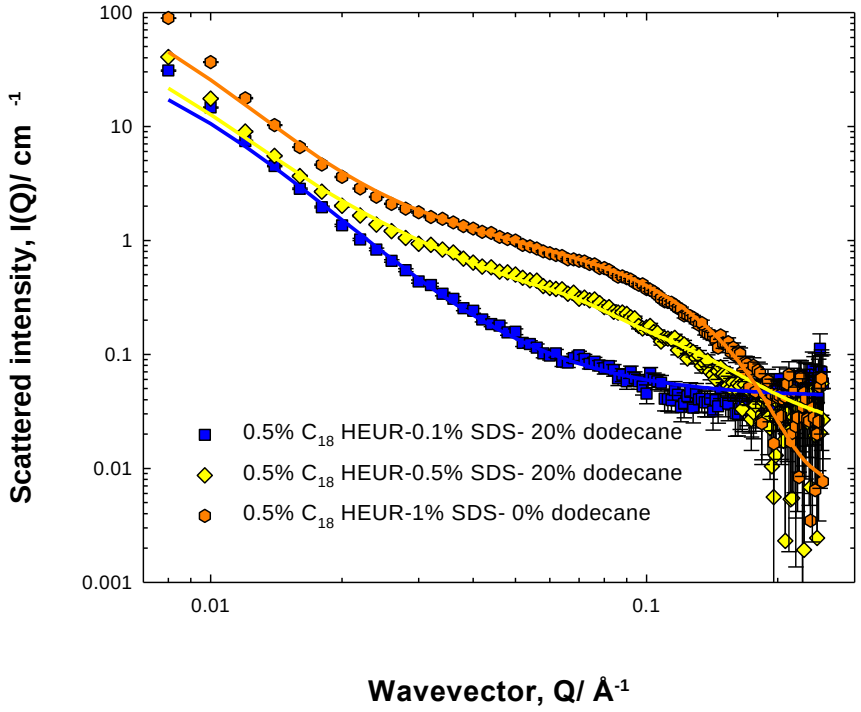
Scattered intensity, I(Q)/ cm -1
100
10
1
0.1
0.01
0.001
0.01
0.1
0.5% C18 HEUR-0.1% SDS- 20% dodecane
0.5% C18 HEUR-0.5% SDS- 20% dodecane
0.5% C18 HEUR-1% SDS- 0% dodecane
Wavevector, Q/ Å-1

Bottom row

(a)

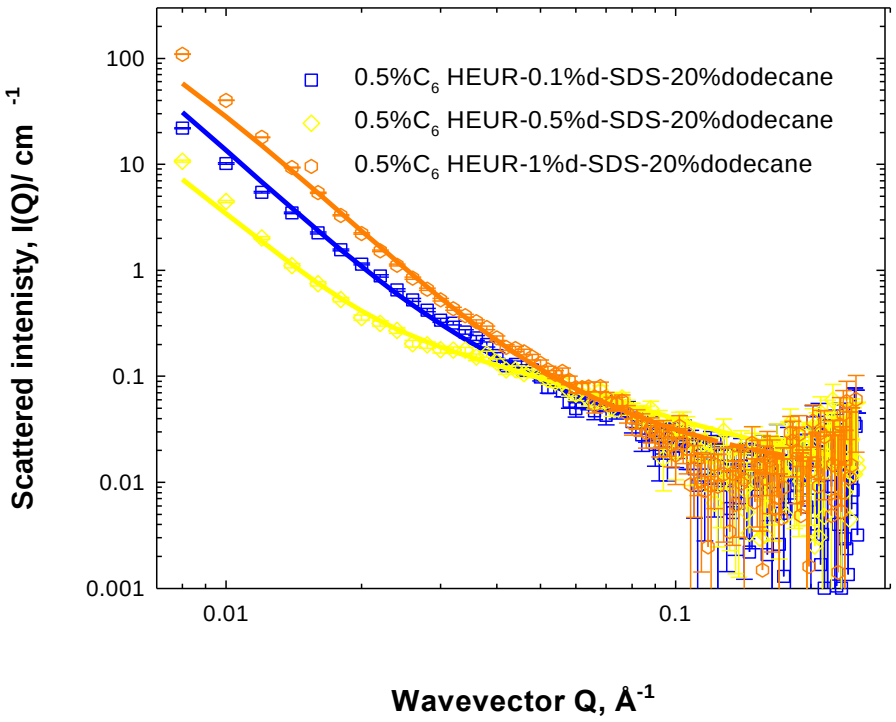
100
10
1
0.1
0.01
0.001
0.01
0.1
0.5%C6 HEUR-0.1%d-SDS-20%dodecane
0.5%C6 HEUR-0.5%d-SDS-20%dodecane
0.5%C6 HEUR-1%d-SDS-20%dodecane
Scattered intenisty, I(Q)/ cm -1
Wavevector Q, Å-1

(b)

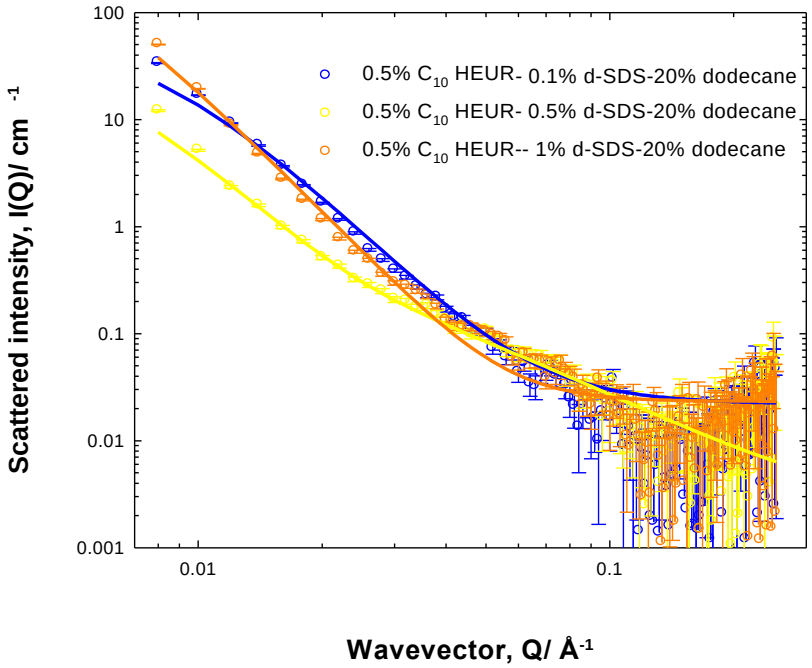
100
10
1
0.1
0.01
0.001
0.01
0.1
0.5% C10 HEUR- 0.1% d-SDS-20% dodecane
0.5% C10 HEUR- 0.5% d-SDS-20% dodecane
0.5% C10 HEUR-- 1% d-SDS-20% dodecane
Scattered intensity, I(Q)/ cm -1
Wavevector, Q/ Å-1

(c)

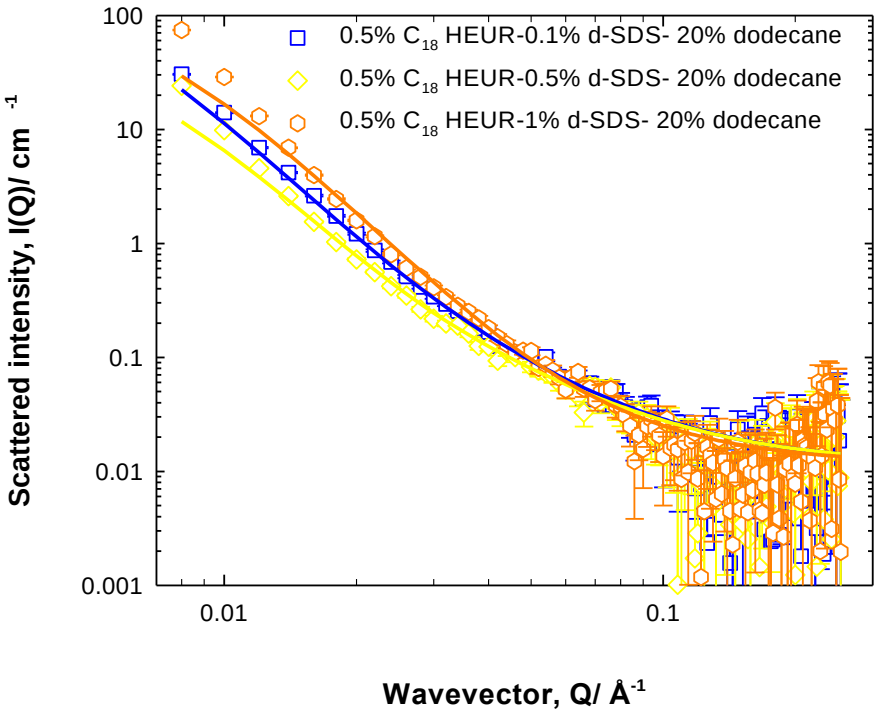
0.5% C18 HEUR-0.1% d-SDS- 20% dodecane
0.5% C18 HEUR-0.5% d-SDS- 20% dodecane
0.5% C18 HEUR-1% d-SDS- 20% dodecane
Scattered intensity, I(Q)/ cm -1
Wavevector, Q/ Å-1
100
10
1
0.1
0.01
0.001
0.01
0.1

References

1. Mancuso JR, McClements DJ, Decker EA. The effects of surfactant type, pH, and chelators on the oxidation of salmon oil-in-water emulsions. *J Agric Food Chem*. **1999**; *47*(10):4112–4116.

2. Zaki NN. Surfactant stabilized crude oil-in-water emulsions for pipeline transportation of viscous crude oils. *Colloids Surfaces A Physicochem Eng Asp*. **1997**;*125*(1):19–25.

3. Church J, Paynter DM, Lee WH. In Situ Characterization of Oil-in-Water Emulsions Stabilized by Surfactant and Salt Using Microsensors. *Langmuir*. **2017**;*33*(38):9731–9.

4. Qian C, McClements DJ. Formation of nanoemulsions stabilized by model food-grade emulsifiers using high-pressure homogenization: Factors affecting particle size. *Food Hydrocoll*. **2011**;*25*(5):1000–1008.

5. Cheetangdee N, Fukada K. Protein stabilized oil-in-water emulsions modified by uniformity of size by premix membrane extrusion and their colloidal stability. *Colloids Surfaces A Physicochem Eng Asp*. **2012**;*403*:54–61.6. Dickinson E. Hydrocolloids as emulsifiers and emulsion stabilizers. *Food Hydrocoll*. **2009**;*23*(6):1473–1482.

7. Ashby NP, Binks BP. Pickering emulsions stabilised by Laponite clay particles. *Phys Chem Chem Phys*. **2000**;*2*(24):5640–5646.

8. Binks BP, Lumsdon SO. Pickering emulsions stabilized by monodisperse latex particles: Effects of particle size. *Langmuir*. **2001**;*17*(15):4540–4547. 9. Chevalier Y, Bolzinger MA. Emulsions stabilized with solid nanoparticles:

Pickering emulsions. *Colloids Surfaces A Physicochem Eng Asp*. **2013**;*439*:23–34.

10. Filali M, Aznar R, Svenson M, Porte G, Appell J. Swollen Micelles Plus Hydrophobically Modified Hydrosoluble Polymers in Aqueous Solutions: Decoration versus Bridging. A Small Angle Neutron Scattering Study. *J Phys Chem B*. **1999**;*103*(34):7293–301.

11. Bagger-Jorgensen H, Coppola L, Thuresson K, Olsson U, Mortensen K. Phase behavior, microstructure, and dynamics in a nonionic microemulsion on addition of hydrophobically end-capped poly(ethylene oxide). *Langmuir*. **1997**;*13*(16):4204–4218.

12. Causse J, Oberdisse J, Jestin J, Lagerge S. Small-angle neutron scattering study of solubilization of tributyl phosphate in aqueous solutions of L64 pluronic triblock copolymers. *Langmuir*. **2010**;*26*(20):15745–15753.

13. Stieber F, Eicke HF. Solution of telechelic ionomers in water/AOT/oil (w/o) microemulsions: a static and dynamic light scattering study. *Colloid & Polym Sci.* **1996**;*274*(9):826–835.

14. Struis RPWJ, Eicke HF. Polymers in complex fluids: Dynamic and equilibrium properties of nanodroplet-ABA block copolymer structures. *J Phys Chem.* **1991**;*95*(15):5989–5996.

15. Parihar SK, Goswami AK, Raina AM. Stabilization of o/w emulsions by polymer surfactant mixture. *Int J Chem Sci.* **2008**;*6*(1):205–211.

16. Abrahmsen-Alami S, Stilbs P. NMR Self-Diffusion of associative polymers in aqueous solution: The influence of the hydrocarbon end-chain length on the

polymer transport dynamics in single-and two-component mixtures. *J Colloid Interface Sci.* **1997**;*189*(1):137–143.

17. Claridge TDW. High-Resolution NMR Techniques in Organic Chemistry. Second Edition. Oxford,UK: *Elsevier*; **2009**.

18. Heenan RK, King SM, Turner DS, Treadgold JR. SANS2d at the ISIS second target station. 17th Meet Int Collab Adv Neutron Sources. **2005**;1–6. Available from: http://www.isis.stfc.ac.uk/instruments/sans2d/publications/sans2d-at-isis10323.pdf (accessed January 2016).

19. Suzuki S, Uneyama T, Inoue T, Watanabe H. Nonlinear rheology of telechelic associative polymer networks: Shear thickening and thinning behavior of hydrophobically modified ethoxylated urethane (HEUR) in aqueous solution. *Macromolecules*. **2012**;*45*(2):888–98.

20. Zhang K, Xu B, Winnik MA, Macdonald PM. Surfactant interactions with HEUR associating polymers. *J Phys Chem*. **1996**;*100*(23):9834–9841.

21. Ibrahim MS, Valencony J, King S, Murray M, Szczygiel A, Alexander BD, Griffiths PC. Studying the interaction of hydrophobically modified ethoxylated urethane (HEUR) polymers with sodium dodecylsulfate (SDS) in concentrated polymer solutions. *J Colloid Interface Sci* . **2018**;*529*:588–598.

22. Ibrahim MS, Rogers S, Mahmoudy N, Murray M, Szczygiel A, Green B, et al. Surfactant modulated interaction of hydrophobically modified ethoxylated urethane (HEUR) polymers with impenetrable surfaces. *J Colloid Interface Sci*. **2018**;*539*:126–34.

23. Stilbs P, Paulsen K, Griffiths PC. Global least-squares analysis of large, correlated spectral data sets: application to component-resolved FT-PGSE NMR spectroscopy. *J Physical Chemistry* **1996;***100*:8180-8189.

24. Gupta SS, Ghosh M. Formulation development and process parameter optimization of lipid nanoemulsions using an alginate-protein stabilizer *J Food Sci Technol.* **2015**; 52(5): 2544–2557.

25. Wang J, Shi A, Agyei D, Wang Q. Formulation of water-in-oil-in-water (W/O/W) emulsions containing trans-resveratrol *RSC Adv.*, **2017**; 7: 35917-35927

26. Marquez R, Forgiarini AM, Langevin D. Instability of Emulsions Made with Surfactant–Oil–Water Systems at Optimum Formulation with Ultralow Interfacial Tension *Langmuir* **2018**; 34(31): 9252–9263